A Free-Piston Stirling Cooling Prototype for Ultra-Low Temperature Freezing

K.Q. Luo[1, 2], Y.L. Sun[1, 2], Z.J. Jiang[1,2], E.C. Luo[1, 2], J.Y. Hu[1, 2], L.M. Zhang[1], Z.H. Wu[1], Z.L. Jia[1, 2], Y. Zhou[1, 2]

[1] Key Laboratory of Cryogenics, Technical Institute of Physics and Chemistry, Chinese Academy of Sciences, Beijing, China 100190
[2] University of Chinese Academy of Sciences, Beijing, China 100049

ABSTRACT

In recent years, the demand for ultra-low temperature freezer has been growing rapidly. It can not only be used for the preservation of some special food, but also be popularly utilized in biological storage. Due to the outstanding advantages of environmental-friendly working substance and high energy efficiency, the free-piston Stirling cooler is getting attention for the development for ultra-low temperature freezing. In this paper, the design and construction of a kW-class free-piston Stirling cooling system for ultra-low temperature freezing is described which can operate in the temperature range from -100°C to -60°C. Experimental results show that the system can obtain a maximum cooling capacity of nearly 1000W@-80°C with a corresponding COP around 0.5 under a charging pressure of 3.25 MPa, a working frequency of 50 Hz and a driving pressure ratio of 1.3. As a result, it demonstrates that the free-piston Stirling cooling system has a good potential for achieving high efficiency and large cooling capacity for the ultra-low temperature freezing application.

INTRODUCTION

Generally, the cooling temperature zone below -60℃ is called the ultra-low temperature freezing range [1]. With the development of technology and improvement of standard of living, the demand for ultra-low temperature freezing has received more concern. It can be widely utilized in cyro-preservation of seafood like salmon and tuna, the long-term storage of biological, chemical and medical products such as vaccines and plasma [2, 3].

It is well known that the cooling temperature above -20°C is the typical storage temperature of the household refrigerator, which is also the effective cooling temperature zone of a single-stage vapor compression refrigeration cycle. For ultra-low temperature freezing, the two-stage cascade refrigeration technology is the preferred method for a cooling temperature of about -80°C [4]. For instance, SANYO Corporation in Japan and Thermo Scientific Corporation in the USA have developed several series of commercial ultra-low temperature freezers, which can achieve the cooling temperature below -80°C [5, 6]. In principle, increasing the number of cascade stages can increase the lowest cooling temperature. Due to the increase in cost and complexity, three-stage cascade cycle is relatively rare in practical applications. Moreover, the mixed-gases Joule-Thomson refrigeration technology is also used for ultra-low temperature freezing [7]. For example, MEILING Corporation in China has exploited the products by developing single-stage mixed-gases Joule-Thomson cooling technology with a simpler system configuration [8]. However, these refrigeration technologies need to take into serious consideration the refrigerants' selection to avoid the greenhouse effect, ozone depletion and other environmental safety problems.

Among the outstanding advantages of compact configuration, high efficiency and environmental-friendly working substance, free-piston Stirling cooling technology is considered an effective alternative to the above-mentioned technologies. With respect to the development of free-piston Stirling cooler, it was mainly focus on the cryogenic temperature refrigeration in the early period, especially for the refrigeration in liquid nitrogen temperature zone [9]. In the past two decades, the free-piston Stirling coolers were developed for higher temperature cooling in the room-temperature range with larger cooling capacity. Besides, several corporations have already developed the ultra-low temperature freezers like Stirling Ultracold Corporation in the USA and Twinbird Corporation in Japan [10, 11]. In 2012, D.M. Berchowitz et al. analyzed and compared the performances of a commercialized free-piston Stirling ultra-low temperature freezer with a two-stage cascade system operating at the cooling temperature of -90℃ [12]. His report showed that the free-piston Stirling cooler could obtain a substantially increased COP of about 0.39, which was also the highest COP being reported.

In this paper, the experimental results of an effective free-piston Stirling cooling system are carried out in detail. The reported results demonstrate good potential in the ultra-low temperature freezing application.

EXPERIMENTAL SYSTEM SETUP

System Configuration

The experimental system consists of two main subsystems, including the dual-opposed type linear compressor and the free-piston Stirling cooler (FPSC), which is shown in Figure 1. The linear compressor is used to drive the free-piston Stirling cooler, which is not specially designed for this cooler yet. Besides, in order to adjust the input electrical power and operating frequency, the linear compressor is controlled by a variable frequency power source. In addition, the core components of the free-piston Stirling cooler are the ambient heat exchanger, regenerator, cold-end heat exchanger and displacer. The structural parameters of each components are listed in Table 1. The regenera-

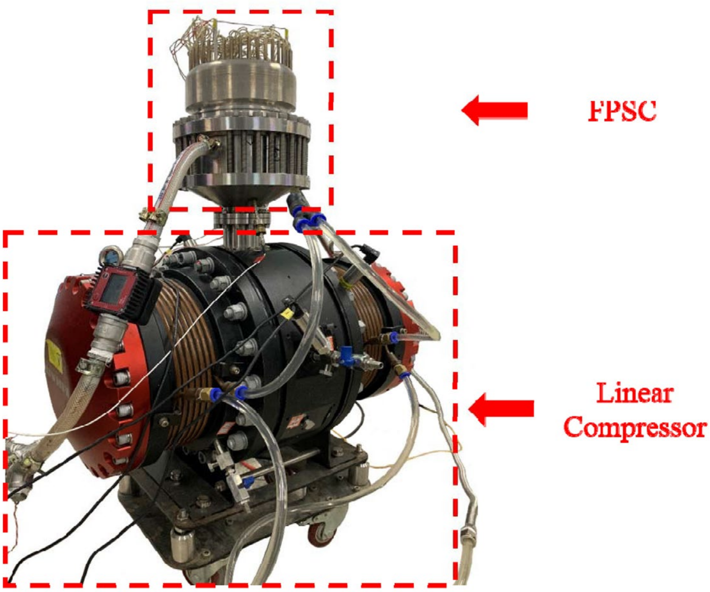

Figure 1. The photograph of the experimental system

Table 1. Main structural parameters of the free-piston Stirling cooler

Component	Specifications	
Compression space	Volume(cc)	452
Ambient heat exchanger	Type	Shell-and-tube
	Length(mm)	63
	Tube diameter (mm)	1.2
	Tube number	648
Regenerator	Outer diameter (mm)	164
	Inner diameter (mm)	124.6
	Length (mm)	39
	Porosity	0.8
	Wire diameter (μm)	50
Cold-end heat exchanger	Type	Finned copper
	Length (mm)	49.8
	Channel width (mm)	0.3
	Chanel number	200
Displacer	Diameter (mm)	120
	Rod diameter (mm)	19.9
	Spring stiffness (kN/m)	200
	Moving mass (kg)	1.8
Expansion space	Volume (cc)	150

tor is the key component for acoustic-to-thermal conversion; and the heat exchangers are used for absorbing or releasing the thermal energy. There are two main functions of the displacer: one is to adjust and match the phase of acoustic impedance based on its mass and spring stiffness, leading to a suitable acoustic field inside the cooler; the other is to recover a portion of acoustic power from the outlet of the cold-end heat exchanger.

The working principle of the entire system is that: the linear compressor converts the input electric power into mechanical energy in the form of acoustic power, in order to drive the FPSC. The acoustic power transfer through the regenerator along the direction of the decreasing temperature gradient consumes a portion of acoustic power to pump heat from the cold-end heat exchanger to the ambient heat exchanger. The acoustic power from the outlet of the cold-end heat exchanger is recovered by the displacer and transfers to the inlet of the ambient heat exchanger together with the acoustic power converted by the linear compressor, thereby operating cyclically.

Experimental Setup and Evaluation

During the experiments, the ambient heat exchanger is cooled by the circulating water at 20°C, while the cold-end heat exchanger is heated by electric heating rods and its cooling capacity is measured by the power meter. The cooling temperature is monitored by three calibrated PT-100 platinum resistance thermometers. Besides, four dynamic pressure sensors are installed in the experimental system to measure the dynamic pressures at two backside cabinets of the linear compressor, the front-side cabinet of the linear compressor and the compression space of the cooler, while the mean working pressure of the experimental system is measured by a static pressure transducer. This data can be used to calculate the acoustic power.

In the following context, several parameters are introduced for evaluating the performance of the entire experimental system.

The input acoustic power of FPSC converted by the linear compressor is calculated as:

$$W_a = \frac{1}{2}\left|\hat{P}_{comp}\right|\left|\hat{U}\right|\cos\theta_{PU} = \frac{\omega V_b \cos\theta_{PU}}{2\gamma P_0}\left|\hat{P}_{comp}\right|\left|\hat{P}_b\right| \tag{1}$$

The coefficient of performance of FPSC based on the input acoustic power is defined as:

$$COP_a = \frac{Q_{cooling}}{W_{a1} + W_{a2}} \tag{2}$$

The relative Carnot efficiency based on the input acoustic power is expressed as:

$$\eta_a = \frac{Q_{cooling}}{W_{a1} + W_{a2}} \left(\frac{T_0 - T_c}{T_c} \right) \tag{3}$$

Generally, the efficiency of the entire system is affected by the efficiency of electric-to-acoustic conversion in the linear compressor and the cooling efficiency of FPSC. As is shown in Eq.(2) and Eq.(3), the efficiency of the linear compressor is ignored. It is due to what is mentioned above: this linear compressor is not designed for this FPSC, the acoustic impedance match between the linear compressor and the cooler is not at an optimal condition. Hence, in this paper, we mainly focus on the performance of the free-piston Stirling cooler.

EXPERIMENTAL RESULTS ANE DISCUSSION

Influences of driving pressure ratio and cooling temperature

In this section, the influences of driving pressure ratio and cooling temperature are investigated in detail. In the experiments, the cooling temperature is fixed at -100°C, -90°C, -80°C, -70°C and -60°C, respectively; while the driving pressure ratio is fixed at 1.15, 1.20, 1.25 and 1.30, respectively.

The performances of the system including the cooling capacity, COP_a, input acoustic power to the FPSC and input electrical power from the compressor under different cooling temperatures and driving pressure ratios are given in Figure 2. As can be seen from Figure 2(a), a higher cooling temperature and a higher driving pressure ratio lead to a larger cooling capacity. Moreover, as the driving pressure ratio increases, the pressure amplitude gradually gets larger, leading to a rising trend

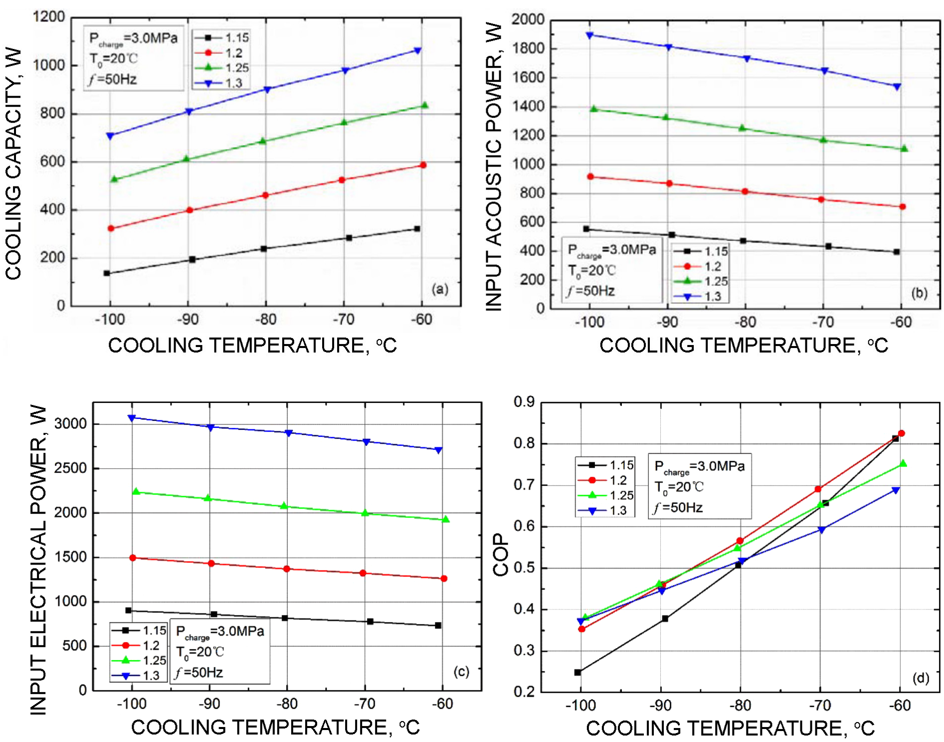

Figure 2. Cooling capacity(a), input acoustic power(b), input electrical power (c) and COP_a(d) vs. cooling temperature under different driving pressure ratios

of the input acoustic power to the FPSC; with the increase of cooling temperature, the temperature difference between the two sides of the regenerator declines and the temperature gradient inside the regenerator decreases, resulting in a decreasing input acoustic power and input electrical power, as are shown in Figures 2(b) and 2(c). Figure 2(d) presents the variation of COP_a under different cooling temperatures and driving pressure ratios. It is noted that the driving pressure ratio doesn't show an obvious influence on the COP_a. The COP_a significantly goes up with the increasing the cooling temperature, relative to the decreasing of input acoustic power. Roughly speaking, as the cooling temperature is fixed at -80°C, the cooling capacity varies from 239W to 903W with the driving pressure ratio increasing from 1.15 to 1.30, with a corresponding COP_a ranging from 0.51 to 0.57.

Influence of charging pressure and operating frequency

Charging pressure and operating frequency are also two key parameters that can affect the performance of FPSC. The variation of charging pressure can change the physical parameters of working substance, such as density, thermal conductivity, viscosity and so on. As for the operating frequency, it can not only determine the mechanical resonant state and phase adjustment of the displacer, but also has influence on the thermal penetration depth and viscous penetration depth. Hence, it's worthy for investigating the impacts of charging pressure and operating frequency. In the experiments, the charging pressure is fixed at 2.75MPa, 3.0MPa and 3.25MPa, respectively; while the operating frequency is fixed at 47.5Hz, 50Hz, 52.5Hz and 55Hz, respectively.

Figures 3(a) and 3(b) show the cooling capacity and COP_a at the cooling temperature of -80°C under different charging pressures and operating frequencies. It is obvious that the higher the charging pressure, the larger the cooling capacity. When the charging pressure goes up to 3.25MPa, the cooling capacity at -80°C can achieve about 963W. On the contrary, the COP_a drops with the increase in charging pressure, probably relating to the flow viscosity and heat transfer. For instance, a COP_a of 0.55 is obtained at the charging pressure of 2.75MPa. Besides, the system obtains its optimal

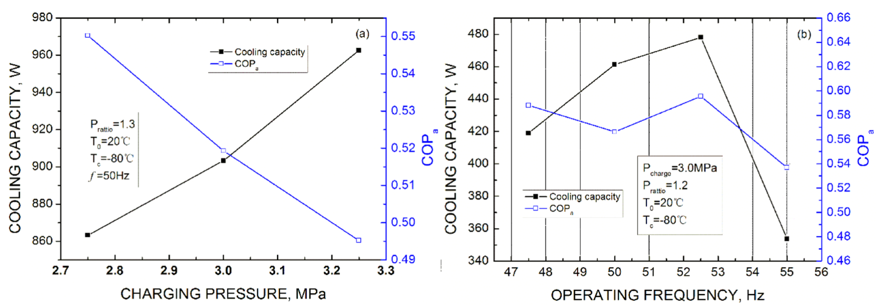

Figure 3. Cooling capacity and COP_a vs. charging pressure(a) and operating frequency (b).

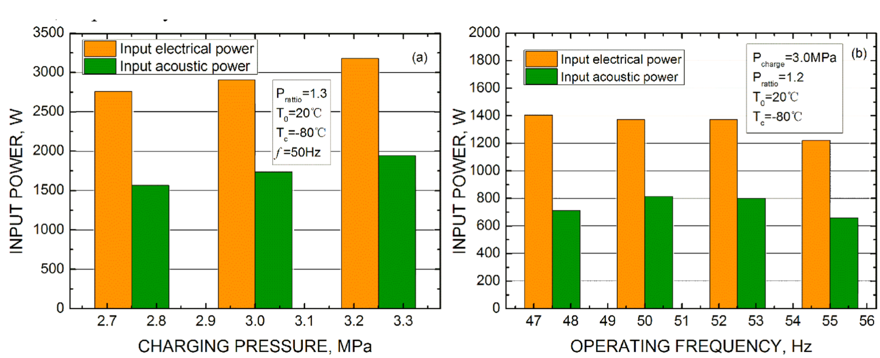

Figure 4. Input acoustic power and electrical power vs. charging pressure(a) and operating frequency(b)

cooling capacity and COP_a under the operating frequency of 52.5Hz. Figures 4(a) and 4(b) give the input acoustic power and electrical power under different charging pressures and operating frequencies. When the charging pressure rises, the pressure amplitude is enhanced as the driving pressure ratio is fixed, resulting in larger input acoustic power and electrical power. In addition, the system gets its highest input acoustic power at an operating frequency of 50Hz, while the input electrical power shows a decreasing trend as the operating frequency rising.

CONCLUSION

In summary, an experimental system of an electric-driven free-piston Stirling cooler was built and tested. Our experimental results show that this cooler was able to obtain nearly 1000W@-80°C with a corresponding COP_a of above 0.5, which is competitively efficient compared with the current conventional technologies. Moreover, considering the environmental-friendly working substance of helium gas used in this system, the free-piston Stirling cooling system is expected to have great prospect for ultra-low temperature freezing.

Furthermore, more systematic simulations will be carried out in the future, in order to investigate the mechanisms of the influences of different operating and structural parameters on the performance of this FPSC system in detail.

ACKNOWLEDGMENT

This research was supported by the National Key Project of Research and Development Plan of China (Contract No.2016YFB0901403), the National Natural Science Foundation of China (Grant No.51876213 and 51976230) and the Strategic Priority Research Programme, CAS (No. XDA21080300).

REFERENCES

1. Adrián Mota-Babiloni, Mahmood Mastani Joybari, Joaquín Navarro-Esbrí et al, "Ultralow-temperature refrigeration systems: Configurations and refrigerants to reduce the environmental impact," *International Journal of Refrigeration*, vol. 111 (2020), pp. 147-158.
2. Tolstorebrov I., Eikevik T.M., Bantle TM., "Effect of low and ultra-low temperature applications during freezing and frozen storage on quality parameters for fish," *International Journal of Refrigeration, vol. 63* (2016), pp. 37-47.
3. Khadatkar R.M., Kumar S., Pattanayak S.C., "Cryofreezing and cryofreezer," *Cryogenics, vol. 44* (2004), pp. 661-678.
4. Yamaguchi H., Niu X.D., Sekimoto K., Neksa P., "Investigation of dry ice blockage in an ultra-low temperature cascade refrigeration system using CO2 as a working fluid," I*nternational Journal of Refrigeration, vol.* 34 (2011), pp. 466-475.
5. http://us.sanyo.com/Biomedical-Preservation
6. http://www.thermoscientific.com
7. Gong M.Q., Wu J.F., Cheng Q.W. et al, "Development of a -186°C cryogenic preservation chamber based on a dual mixed-gases Joule-Thomson refrigeration cycle," *Applied Thermal Engineering, vol.* 36 (2012), pp. 188-192.
8. http://www.zkmeiling.com
9. Zhu S.M., Yu G.Y., Li X.W. et al, "Parametric study of a free-piston Stirling cryocooler capable of providing 350 W cooling power at 80 K," *Applied Thermal Engineering, vol.* 174 (2020), pp. 115101.
10. http://www.stirlingultracold.com/ultra-low-freezers
11. http://fpsc.twinbird.jp/legacy/en/products_application_e.html
12. Berchowitz D.M., Kwon Y., "Environmental Profiles of Stirling-Cooled and Cascade-Cooled Ultra-Low Temperature Freezers," *Sustainability*, vol. 4 (2012), pp. 2838-2851.